Research Square

Preprints are preliminary reports that have not undergone peer review.
They should not be considered conclusive, used to inform clinical practice,
or referenced by the media as validated information.

Channel Characteristics of Long-distance Magnetic Induction based Through-the-earth Communication and Performance Analysis

Chuanxian Ma
Shanxi China Coal Pingshuo Blasting Equipment Co., Ltd
Yanjun Zhu
Shanxi China Coal Pingshuo Blasting Equipment Co., Ltd
Lifeng Sun
Chinese Institute of Coal Science
Baojun Zhu
Shanxi China Coal Pingshuo Blasting Equipment Co., Ltd
Huifeng Cheng
Chinese Institute of Coal Science
Xinlei Jia
Chinese Institute of Coal Science
Yue Wang
133313618150163.com

Chinese Institute of Coal Science
Mengtian Dai
Beijing Jiaotong University
Wei Yang
Beijing Jiaotong University

Article

Keywords:

Posted Date: July 24th, 2026

DOI: https://doi.org/10.21203/rs.3.rs-10363587/v1

License: This work is licensed under a Creative Commons Attribution 4.0 International License.
Read Full License

Additional Declarations: No competing interests reported.

Version of Record: A version of this preprint was published at Scientific Reports on October 20th, 2026. See the published version at https://doi.org/10.1038/s41598-026-76876-0.

Channel Characteristics of Long-distance Magnetic Induction based Through-the-earth Communication and Performance Analysis

Chuanxian Ma[1], Yanjun Zhu[1], Lifeng Sun[2,3], Baojun Zhu[1], Huifeng Cheng[2,3], Xinlei Jia[2,3], Yue Wang[2,3*], Mengtian Dai[4] and Wei Yang[4]

[1] Shanxi China Coal Pingshuo Blasting Equipment Co., Ltd., Anjialing Apartment, Pinglu District, Shuozhou City, Shanxi Province,China.
[2] *Chinese Institute of Coal Science, No. 5 Qingniangou Road, Chaoyang District, Beijing,China.*
[3] *State Key Laboratory of Disaster Prevention and Ecology Protection in Open-Pit Coal Mines, No. 5 Qingniangou Road, Chaoyang District, Beijing,China.*
[4] *School of Electronics and Information Engineering, Beijing Jiaotong University, No.3 Shangyuan Village, Haidian District, Beijing,China.*

*Email: 13331361815@163.com

Abstract: Magnetic induction (MI) based through-the-earth (TTE) communication has low path loss, no multipath effect and stable transmission channel. The generation and propagation of magnetic fields in MI based TTE communication do not have the strict requirements of antenna size than that in electromagnetic wave based TTE communication, which is conducive to achieving bidirectional communication between the ground and underground. An equivalent circuit of the receiving and transmitting circuit has been established for long-distance MI based TTE communication, and the transmission function of MI based TTE communication channel can be characterized using the equivalent circuit of the receiving and transmitting circuit. The noise of receivers of MI based TTE communication mainly includes thermal noise on the receiving circuit and electromagnetic noise in the environment where the receiving coil is located. The noise characteristics of receivers of MI based TTE communication were analyzed. The channel characteristics of MI based TTE communication such as amplitude frequency response, impulse response and bandwidth were analyzed by simulation under different TTE medium parameters and TTE communication distance. The amplitude spectrum of the received signal was compared with the amplitude spectrum of the noise. A simulation platform of MI based TTE communication was built, and the performance with BPSK and QPSK modulation was compared under different TTE medium parameters and TTE communication distance. The maximum modulation order that can be adopted by MI based TTE communication under different TTE medium parameters and TTE communication distance was given. These play an important role in improving the performance of long-distance MI based TTE communication systems.

Introduction: After disasters occur in underground coal mines, conventional communication facilities are vulnerable to damage during accidents, resulting in underground communication breakdowns. This prevents rescuers from accurately acquiring the locations and physical conditions of trapped personnel and hinders underground rescue operations. Accordingly, through-the-earth communication systems capable of wireless communication by directly penetrating strata have become critical equipment for safeguarding the life safety of underground personnel during post-disaster rescue missions. [5-8].

For electromagnetic wave through-the-earth communication, ultra-long wave bands with strong penetration capability are required. However, transmitting ultra-long waves demands transmitting antennas ranging from several kilometers to tens of kilometers in length. Consequently, electromagnetic wave-based through-the-earth wireless communication can only realize unidirectional communication [4-6]. Electromagnetic waves undergo multiple reflections and refractions when passing through multi-layer earth media, which leads to severe multipath effects during the transmission of through-the-earth communication signals [7]. In addition, the propagation of electromagnetic waves in earth media is highly susceptible to variations in formation conductivity, and formations with high conductivity drastically shorten the transmission range of electromagnetic wave signals [8,9].

Magnetic induction (MI) based through-the-earth (TTE) communication adopts magnetic field signals as communication carriers without stringent constraints on antenna size. Transmitting and receiving coils with small radii are more suitable for narrow underground mine environments and facilitate bidirectional communication between the ground and underground workings [10]. Except for magnetic substances such as iron, cobalt and nickel, the magnetic permeability of other strata materials is close to the permeability of free space. Accordingly, magnetic field signals do not refract while propagating in earth media. Furthermore, magnetic fields are solenoidal fields with closed magnetic induction lines, so magnetic induction through-the-earth communication is free of multipath effects and can guarantee the quality of transmitted signals [11,12].

At present, MI based TTE communication has gradually become the mainstream scheme for through-the-earth wireless transmission and attracted extensive research attention. For short-range magnetic induction through-the-earth wireless sensor networks, Reference [13] analyzed the path loss and transmission bandwidth of short-range magnetic induction through-the-earth communication. The analysis elaborately took into account the influences of soil properties, coil radius and turns, coil resistance, operating frequency and other factors on path loss and transmission bandwidth. The analytical results indicate that magnetic induction through-the-earth communication based on direct coupling between transmitting

and receiving coils achieves deeper penetration depth than electromagnetic wave through-the-earth communication, yet with narrower transmission bandwidth. On this basis, Reference [13] further proposed a waveguide-type magnetic induction through-the-earth communication scheme deploying multiple passive relay coils between the transmit and receive coils to realize improved penetration depth and transmission bandwidth.

Different from Reference [13], Reference [14] focuses on digital transmission methods for short-range magnetic induction through-the-earth wireless sensor networks. It also investigates two communication schemes: magnetic induction through-the-earth communication with direct coupling between transmit and receive coils, and waveguide magnetic induction through-the-earth communication equipped with multiple passive relay coils between the transceiving coils. The through-the-earth channel model and noise model under the two schemes are derived in Reference [14]. The performance of magnetic induction through-the-earth communication is analyzed via the signal-to-noise ratio of transmitted digital symbols to explore its optimal modulation scheme. For various types of through-the-earth channels, Reference [14] presents finite-alphabet modulation schemes that minimize the data rate loss.

Aiming at long-distance magnetic induction through-the-earth communication, considering the weak coupling between transmit and receive coils in practical long-range MI-TTE scenarios, Reference [15] proposed a channel capacity analysis method for transceivers equipped with single-axis air-core coils. Simulation results reveal that the channel capacity of long-distance through-the-earth communication decreases remarkably as the transmission distance increases, while the capacity can still reach hundreds to thousands of bits per second (bps) within a penetration range of several hundred meters.

To construct a practical long-distance magnetic induction through-the-earth communication system, this paper establishes the channel transfer function under varying earth medium parameters for long-range MI-TTE communication and analyzes the noise characteristics of the receiver. On this basis, channel characteristics including amplitude-frequency response, impulse response and channel bandwidth of the MI-TTE system are acquired under different earth medium parameters and transmission distances. A simulation platform for magnetic induction through-the-earth communication is developed to compare the communication performance of BPSK and QPSK modulation schemes under diverse medium parameters and penetration distances. Furthermore, the maximum applicable modulation order under various medium parameters and transmission ranges is provided to maximize the data rate of through-the-earth transmission.

MI-TTE Communication System Model: Figure 1 illustrates the long-distance magnetic induction based through-the-earth communication system where both the transmitter (TS) and receiver (RS) adopt single-axis multi-turn air-core coils. The radius and number of turns of the transmit coil are denoted as a_t and n_t, while those of the receive coil are denoted as a_r and n_r.

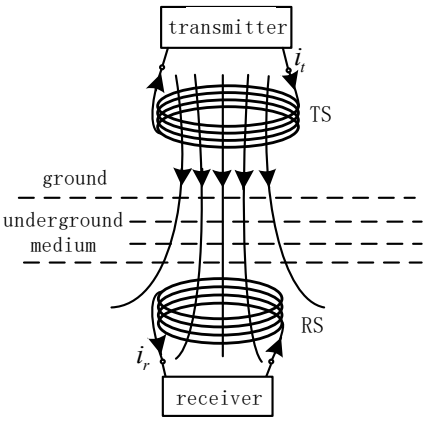


Fig 1 *A schematic diagram of MI-TTE communication system.*

Figure 2 shows the equivalent circuit of the transmitting and receiving loops in the magnetic induction based through-the-earth communication system. In the transmitter equivalent circuit in Figure 2(a), R_t represents the internal resistance of the transmit coil and L_t represents the inductance of the transmit coil, the inductance of the air-core coil is calculated by $L_t = 0.5\mu_0\pi n_t^2 a_t$. In the receiver equivalent circuit in Figure 2(b), the voltage source $u_e$denotes the instantaneous induced electromotive force generated inside the receive coil when alternating magnetic fields pass through it, L_r is the inductance of the receive coil, $L_r = 0.5\mu_0\pi n_r^2 a_r$, R_r is its internal resistance, R_L refers to the load resistance of the receiver, and C_L represents the compensation capacitance matched to the receiver load. Since the receive coil is an inductive component, a compensation capacitor needs to be deployed on the receiver load to achieve maximum power transmission through strata. During the operation of the magnetic induction based through-the-earth communication system, the voltage source $u_s = \sqrt{2}U_S sin(2\pi f t)$ at the front end of the transmitter generates alternating current i_t on the transmitting loop, which excites an alternating magnetic field. U_S is the effective value of u_s and f is the operating frequency of u_s. When this alternating magnetic field penetrates stratum media and crosses the plane of the receive coil, induced electromotive force u_e will be generated inside the receive coil and further induce alternating current i_r on the receiving loop. The induced current i_r flows through the load resistance R_L and produces a voltage u_r across its two

terminals,and the receiving circuit realizes magnetic induction through-the-earth communication by detecting the voltage on the receiver load.

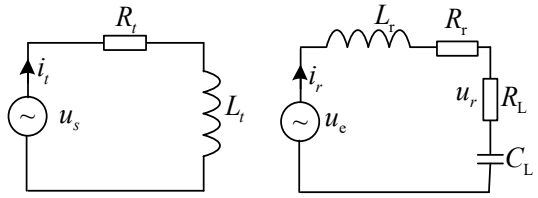


Fig 2 *The equivalent circuitry of transceivers: (a) Transmit loop and (b) Receive loop.*

To calculate the vector value of magnetic induction intensity penetrating through strata, a coordinate system as illustrated in Figure 3 is established for the through-the-earth communication system shown in Figure 1. In Figure 3, the planes of both transmit and receive coils are parallel to the ground. A three-dimensional Cartesian coordinate system is constructed with the center O of the transmit coil (TS) as the origin, the plane of the transmit coil as the XOY plane, and the central axis of the coil as the Z-axis. Point C denotes an arbitrary point on the transmit coil. Since the height of the transmit coil is far smaller than its radius and the through-the-earth communication distance, point C is assumed to always lie within the XOY plane. The center of the receive coil is located at point Q, which is directly beneath point O. The distance between O and Q is denoted as r, and the distance between point C and point Q is denoted as r'. Additionally, a_t represents the radius of the transmit coil, and a_r represents the radius of the receive coil.

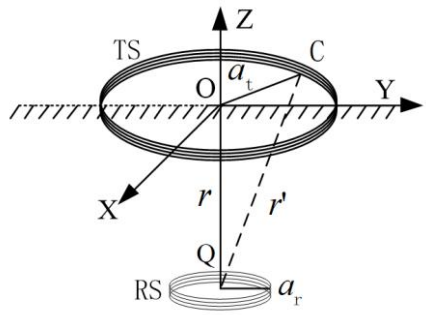


Fig 3 *Coordinate model of TTE communication system.*

Neglecting the eddy current effect, the magnetic induction intensity generated at point Q by the infinitesimal element $\boldsymbol{e}_l dl$ at point C on the transmit coil is expressed in Equation (1) according to the Biot-Savart Law.

$$d\boldsymbol{B} = \frac{n_t \mu_0 \mu_r i_t}{4\pi} \cdot \frac{\boldsymbol{e}_l dl \times \boldsymbol{r}'}{r'^3} \tag{1}$$

In the formula, $\boldsymbol{e}_l$ denotes the unit direction vector of current, $\boldsymbol{r}'$ represents the distance vector between point C on the coil and point Q, $r' = |\boldsymbol{r}'|$, μ_r stands for the relative permeability of stratum media, and μ_0 refers to the permeability of free space. The total magnetic induction intensity at point Q equals the vector superposition of magnetic induction intensities generated by all infinitesimal elements on the transmit coil at point Q. Since the through-the-earth communication distance r is much larger than the radii of the transmit and receive coils, $\boldsymbol{r}'$ can be approximated as the distance vector $\boldsymbol{r}$ from the center of the transmit coil to point Q.

Integrating Equation (1) along the entire circular arc of the transmit coil TS, the through-the-earth magnetic induction intensity $\boldsymbol{B}_Q$ at point Q can be derived as shown in Equation (2).

$$\boldsymbol{B}_Q = \oint \frac{n_t \mu_0 \mu_r i_t}{4\pi} \cdot \frac{\boldsymbol{e}_l dl \times \boldsymbol{r}'}{r'^3} \tag{2}$$

To achieve optimal signal reception, the receiver coil RS is placed directly beneath the transmit coil TS in the communication system. Accordingly, the magnitude of the through-the-earth magnetic induction intensity at point Q is given by Equation (3).

$$|\boldsymbol{B}_Q| = \frac{n_t \mu_0 \mu_r i_t a_t^2}{2r^3} \tag{3}$$

In practical scenarios, the alternating magnetic field generated by the transmit coil will induce eddy currents while penetrating strata, which leads to the attenuation of the through-the-earth alternating magnetic field [16]. Therefore, the actual magnitude of the through-the-earth magnetic induction intensity at point Q is expressed in Equation (4) [15].

$$|\boldsymbol{B}_Q| = \frac{n_t \mu_0 \mu_r i_t a_t^2}{2r^3} \cdot e^{-r\sqrt{\pi f \mu_0 \mu_r \sigma}} \tag{4}$$

Through-the-earth Channel Transfer Function: The magnetic induction through-the-earth channel can be characterized by the through-the-earth channel transfer function $H(f)$ [17]. This transfer function enables the analysis of channel

characteristics including amplitude-frequency response, impulse response and bandwidth of the through-the-earth communication system under various earth media and transmission distances. On this basis, further analysis can be conducted on system performance metrics such as bit error rate and data transmission rate of the through-the-earth communication system.

In the transmitting loop shown in Figure 2(a), the effective value I_t of the current i_t in the equivalent circuit can be derived as Equation (5) from the voltage u_s of the voltage source at the front end of the transmitter.

$$I_t = |i_t| = \left|\frac{u_s}{R_t + j2\pi f L_t}\right| = \frac{U_S}{\sqrt{R_t^2 + (j2\pi f L_t)^2}} \tag{5}$$

Then the instantaneous current i_t in the equivalent circuit is expressed by Equation (6).

$$i_t = \frac{u_s}{R_t + j2\pi f L_t} = \frac{\sqrt{2}U_S}{\sqrt{R_t^2 + (j2\pi f L_t)^2}} sin\left[2\pi f t + arctan(\frac{-2\pi f L_t}{R_t})\right] \tag{6}$$

In the receiving loop illustrated in Figure 2(b), u_e denotes the induced electromotive force generated inside the receive coil. Let Φ be the magnetic flux passing through a single receive coil, according to Faraday's Law of Electromagnetic Induction, the relationship is expressed as Equation (7).

$$u_e = n_r \frac{d\Phi}{dt} = n_r \frac{d(\int_S \boldsymbol{B}_Q \cdot \boldsymbol{e}_n dS)}{dt} = \frac{\sqrt{2} I_t \pi^2 f n_t n_r \mu_0 \mu_r a_t^2 a_r^2}{r^3} cos(2\pi f t + \varphi_i) \cdot e^{-r\sqrt{\pi f \mu_0 \mu_r \sigma}} \tag{7}$$

In the formula, $\boldsymbol{e}_n$ represents the unit vector perpendicular to the plane of the transmit coil, $\varphi_i = arctan(\frac{-2\pi f L_t}{R_t})$, and S denotes the area of a single receive coil. Since the radius of the receive coil is negligible compared with the through-the-earth transmission distance, the magnetic induction intensity penetrating the receive coil is regarded as uniform and equal to $\boldsymbol{B}_Q$ given in Equation (4).

The effective value U_e of u_e can be obtained from Equation (8) by rearranging Equation (7).

$$U_e = \frac{I_t \pi^2 f n_t n_r \mu_0 \mu_r a_t^2 a_r^2}{r^3} \cdot e^{-r\sqrt{\pi f \mu_0 \mu_r \sigma}} \tag{8}$$

Therefore, the effective value I_r of the induced current i_r on the receive coil can be expressed as Equation (9).

$$I_r = \frac{U_e}{\sqrt{(R_L + R_r)^2 + (2\pi f L_r - \frac{1}{2\pi f C_L})^2}} = \frac{I_t \pi^2 f n_t n_r \mu_0 \mu_r a_t^2 a_r^2}{r^3 \sqrt{(R_L + R_r)^2 + (2\pi f L_r - \frac{1}{2\pi f C_L})^2}} \cdot e^{-r\sqrt{\pi f \mu_0 \mu_r \sigma}} \tag{9}$$

Based on the equivalent circuits of the transmit and receive loops for the magnetic induction through-the-earth communication system shown in Figure 2, the transfer function of the magnetic induction through-the-earth channel can be written as Equation (10).

$$H(f) = \frac{U_r(f)}{U_s(f)} = \frac{I_r(f) R_L}{U_s(f)} \tag{10}$$

In the formula, $U_s(f)$, $U_r(f)$ and $I_r(f)$ denote the effective values corresponding to u_s, u_r and i_r when the carrier frequency of the through-the-earth communication system is f.

Substituting Equation (5) and Equation (9) into Equation (10), the through-the-earth channel transfer function $H(f)$ of the magnetic induction through-the-earth communication system can be derived as Equation (11).

$$H(f) = \frac{\frac{I_t \pi^2 f n_t n_r \mu_0 \mu_r a_t^2 a_r^2 e^{-r\sqrt{\pi f \mu_0 \mu_r \sigma}}}{r^3 \sqrt{(R_L + R_r)^2 + (2\pi f L_r - \frac{1}{2\pi f C_L})^2}} \cdot R_L}{U_s} = \frac{\pi^2 f n_t n_r \mu_0 \mu_r a_t^2 a_r^2 R_L \cdot e^{-r\sqrt{\pi f \mu_0 \mu_r \sigma}}}{r^3 \sqrt{R_t^2 + (2\pi f L_t)^2} \cdot \sqrt{(R_L + R_r)^2 + (2\pi f L_r - \frac{1}{2\pi f C_L})^2}} \tag{11}$$

The near-field through-the-earth communication of magnetic induction through-the-earth channel under strong coupling conditions exhibits the frequency splitting effect, with two or more resonant frequency points appearing [18]. However, for long-distance magnetic induction through-the-earth communication scenarios, the coupling between transmit and receive coils is weak. The through-the-earth channel transfer function $H(f)$ only has a single maximum value at the resonant frequency point. This indicates that when the transmission distance is relatively large in long-distance magnetic induction through-the-earth communication, the coupling between transmit and receive coils is extremely weak, and the frequency splitting phenomenon will not occur.

Channel Noise Characteristics: The magnetic field signal in magnetic induction through-the-earth communication attenuates rapidly with the increase of transmission distance. After propagating through hundreds of meters of stratum, the magnetic induction intensity of the received signal underground becomes extremely weak, and the induced electromotive force on the receive coil is also very small. Therefore, even minor noise can severely interfere with signal reception of the magnetic induction through-the-earth communication system, reducing the signal-to-noise ratio (SNR) of the received signal and increasing the bit error rate (BER) of the through-the-earth communication system. To evaluate the relationship between the bit error rate performance of the magnetic induction through-the-earth communication system and parameters including transmission distance, data rate and modulation scheme, it is necessary to analyze and characterize the noise characteristics of the through-the-earth communication system.

The noises that degrade signal reception in magnetic induction through-the-earth communication systems mainly include thermal noise generated by the receiving circuit and electromagnetic noise from the ambient environment

surrounding the receive coil. The power spectral density of thermal noise within the receiving loop is given by Equation (12) [19].

$$E\{|U_{nr}(f)|^2\} = 4KT(R_r + R_L) \tag{12}$$

The electromagnetic noise in the environment where the receive coil of the magnetic induction through-the-earth communication system is located mainly refers to the electromagnetic background noise in the roadway surrounding the underground receiver. Overall, this noise approximately follows a Gaussian distribution, and its equivalent power spectral density is expressed as Equation (13) [20].

$$E\{|U_{na}(f)|^2\} = 4KTR_rF_a(f)\phi^2\frac{k_0Z_0}{6\pi} \tag{13}$$

$$\phi^2 = \frac{L_r a_r^3 \pi^2}{R_r \mu_0 ln(\frac{8a_r}{w} - 2)} \tag{14}$$

In the formula, $k_0 = 2\pi f/c$ denotes the wave number of the transmitted signal, c represents the speed of light in vacuum, $Z_0 \approx 377\Omega$ stands for the free-space impedance, ϕ is the quality factor of the antenna, and w refers to the wire diameter of the copper wire for the receive coil. $F_a(f)$ is the environmental noise temperature ratio, whose approximate expression is given by Equation (15).

$$F_a(f) = (294.15 - 36log_{10}f)dB \tag{15}$$

The noise power on the receiver load is the superposition of thermal noise power from the receiving circuit and electromagnetic noise power originating from the environment of the receive coil. Since the receiving loop is not purely resistive, the noise power received across the load resistance is complex power, and its real part represents the average noise power on the receiving load [13], as shown in Equation (16).

$$\begin{aligned} E\{P_n(f)\} &= E\{P_{nr}(f)\} + E\{P_{na}(f)\} \\ &= E\left\{Re\left\{\frac{U_{nr}^2(f)\cdot R_L}{\left|R_r + R_L + j2\pi fL_r + \frac{1}{j2\pi fC_L}\right|^2}\right\}\right\} + E\left\{Re\left\{\frac{U_{na}^2(f)\cdot R_L}{\left|R_r + R_L + j2\pi fL_r + \frac{1}{j2\pi fC_L}\right|^2}\right\}\right\} \\ &= 4KTR_L\int_B \frac{(R_r + R_L + R_rF_a(f)\phi^2\frac{k_0Z_0}{6\pi})}{(R_r + R_L)^2 + (2\pi fL_r - \frac{1}{2\pi fC_L})^2}df \end{aligned} \tag{16}$$

In addition, the power spectral density $E\{|U_n(f)|^2\}$ of noise on the receiving load can also be derived as Equation (17).

$$E\{|U_n(f)|^2\} = E\{|U_{nr}(f)|^2\} + E\{|U_{na}(f)|^2\} = \frac{4KTR_L(R_r + R_L + R_rF_a(f)\phi^2\frac{k_0Z_0}{6\pi})}{(R_r + R_L)^2 + (2\pi fL_r - \frac{1}{2\pi fC_L})^2} \tag{17}$$

Simulation and Analysis: Simulation and analysis are carried out to investigate the characteristics of magnetic induction through-the-earth channels under different formation medium parameters and transmission distances. In the simulation, the radius of the transmit coil a_t is set to 1 m with a turn number n_t of 1000. The receive coil has a radius a_r of 10 cm and 200 turns. Copper wires with diameters of 0.4 mm and 0.14 mm are adopted for the transmit and receive coils, whose unit resistances are 0.128Ω/m and 1.2Ω/m, respectively. The relative permeability of the stratum μ_r equals 1, and the vacuum permeability $\mu_0 = 4\pi \times 10^{-7}T \cdot m/A$ is set to 1.

Figure 4(a) plots the amplitude-frequency characteristic curves of the through-the-earth channel under a transmission distance of 200 m with soil moisture contents of 0%, 25%, 50% and 75%, respectively. For intuitive comparison, the normalized results are presented in Figure 4(b). It can be observed from Figure 4(a) that the channel attenuation of magnetic induction through-the-earth communication increases remarkably with rising soil moisture. For instance, as the soil moisture rises from 0% to 75%, the channel transfer function $H(f)$ attenuates from 1.9×10^{-10} to 4.5×10^{-11}. This indicates that through-the-earth propagation media with higher conductivity introduce drastically enhanced eddy current loss in the channel. By comparing the normalized amplitude-frequency responses of the transfer function in Figure 4(b), it is found that the resonant frequency corresponding to the maximum amplitude of the transfer function is barely affected by soil moisture of the propagation medium. Nevertheless, the channel bandwidth declines as soil moisture increases. Specifically, when soil moisture grows from 0% to 75%, the 3 dB channel bandwidth decreases from approximately 4.3 kHz to around 3.5 kHz.

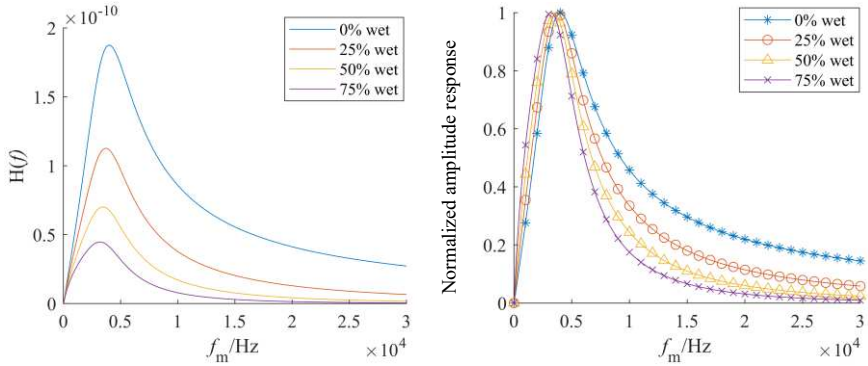


Fig 4 *Amplitude-frequency characteristics of magnetic induction TTE communication channels under different soil moisture: (a) Channel amplitude-frequency characteristics and (b) Normalized channel amplitude-frequency characteristics.*

No closed-form solution can be derived for the time-domain impulse response of the magnetic induction through-the-earth channel. Nevertheless, the time-domain impulse response of the through-the-earth channel can be obtained by performing the inverse Fourier transform on the channel transfer function $H(f)$ followed by normalization, as illustrated in Figure 5. It can be observed from Figure 5 that multipath propagation does not exist in this channel, so the magnetic induction through-the-earth channel is free of delay spread. However, the transmit and receive resonant loops exhibit frequency-selective characteristics and contain energy storage components such as inductors and capacitors, which cause the time-domain impulse response of the magnetic induction through-the-earth channel to feature a long time tail.As shown in Figure 5, the time tail of the channel impulse response is barely affected by the propagation medium. Accordingly, when designing the data rate and modulation scheme of the through-the-earth communication system, dedicated inter-symbol interference mitigation processing tailored to different transmission media is generally unnecessary.

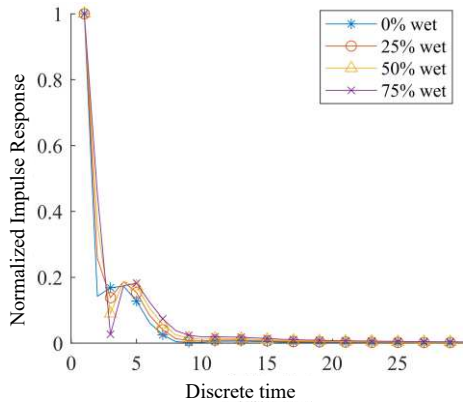


Fig 5 *Normalized channel impulse response.*

Figure 6 presents the simulated amplitude spectra of the received signal and noise under various soil moisture contents at a transmission distance of 200 m. The left vertical axis corresponds to the amplitude spectrum of the received signal, while the right vertical axis denotes the amplitude spectrum of noise. It can be seen from Figure 6 that the noise captured by the magnetic induction through-the-earth communication receiver is also affected by the resonant loops, which agrees with the analytical results derived from Equation (16). Specifically, the noise amplitude reaches its maximum at the resonant frequency and decreases at frequencies far away from the resonant point. Nevertheless, as the frequency deviates from the resonant frequency, the noise amplitude of the receiving loop decays much more slowly and exhibits a flatter profile compared with the received signal amplitude. This characteristic exerts a certain influence on the signal-to-noise ratio performance of the received through-the-earth signal.

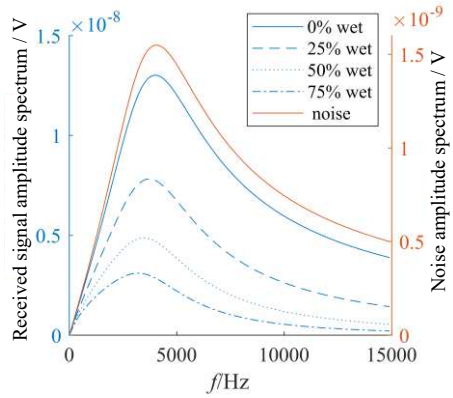


Fig 6 *Spectrum of received signal amplitude and noise amplitude under 200m.*

Figure 7 illustrates the simulated curves of received SNR versus transmission distance under various soil moisture contents. It can be observed that within the transmission distance range of 150 m to 450 m, the received SNR of the magnetic induction through-the-earth communication system attenuates as both the propagation distance and soil moisture increase. At a transmission distance of 150 m, the received SNR reaches 53 dB, 47 dB, 40 dB and 34 dB corresponding to soil moisture contents of 0%, 25%, 50% and 75%, respectively. Accordingly, high-order modulation can be adopted to improve the transmission rate of the through-the-earth communication system under short-distance propagation conditions. When the transmission distance extends to 450 m, the received SNR drops to -3.8 dB, -24 dB, -44 dB and -63 dB for soil moisture of 0%, 25%, 50% and 75%. Compared with the results at 150 m, the SNR decays more rapidly with the increase of transmission distance under higher soil moisture.

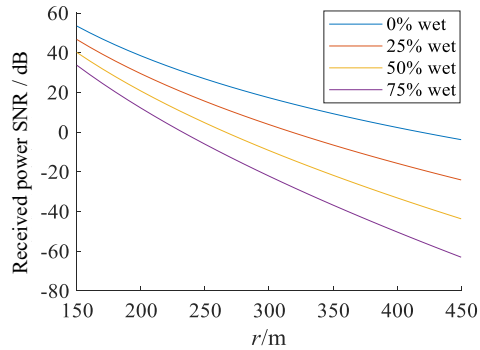


Fig 7 *Relationship between received signal-to-noise ratio and communication distance under different soil moisture.*

Modulation Schemes and Data Rates: For long-distance magnetic induction through-the-earth communication, the transmitted information includes sensor data, text, voice, as well as images and videos. A higher data rate corresponds to stronger information transmission capacity. When the propagation distance is large, the SNR at the underground receiver is extremely low. Adopting high-order modulation with a high data rate will severely degrade the BER performance. Therefore, it is necessary to investigate the maximum achievable transmission rate or modulation order supported by the through-the-earth channel under a target BER constraint.

To verify and compare the communication performance of long-distance magnetic induction through-the-earth communication systems under different modulation schemes, a simulation platform for the through-the-earth communication system is constructed, and its structure is shown in Figure 8. Referring to the simulation and analysis results presented in Section 4, the carrier frequency is set to 4 kHz and the channel bandwidth of the through-the-earth channel is 3.5 kHz. A square-root raised cosine filter with a roll-off factor of 0.5 is adopted as the baseband shaping filter. The attenuation of the through-the-earth channel is calculated based on the channel transfer function $H(f)$, and the receiver noise is generated according to the noise power spectral density $E\{|U_n(f)|^2\}$. Coherent demodulation is employed at the receiving terminal. The relationship between the information rate R_b and channel bandwidth B can be expressed by Equation (18), where α denotes the filter roll-off factor and η represents the spectral efficiency. The source information rate is set to 2.3 kbps for BPSK modulation and 4.6 kbps for QPSK modulation.

$$R_b = \frac{2\eta}{1+\alpha} B \tag{18}$$

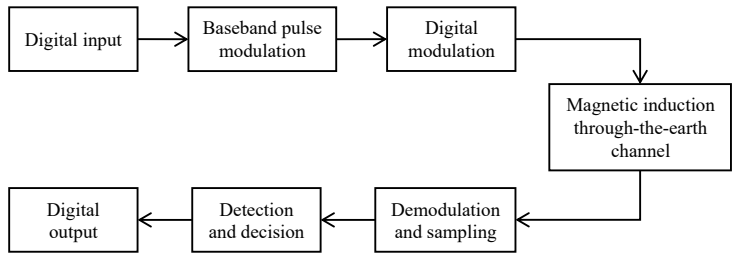


Fig 8 *Signal modulation scheme of magnetic induction TTE communication system.*

Figure 9 shows the simulated BER performance of the magnetic induction through-the-earth communication system with BPSK and QPSK modulation schemes when the transmission distance varies from 150 m to 700 m under different soil moisture contents. It can be observed that under any soil moisture condition, the communication reliability of the system with BPSK modulation is consistently superior to that with QPSK modulation.Given a target BER threshold $SER_t \leq 10^{-3}$, the maximum transmission distance supported by BPSK is approximately 19 m, 11 m, 9 m and 7 m longer than that of QPSK at soil moisture contents of 0%, 25%, 50% and 75%, respectively.In addition, Figure 9 reveals that the maximum communication depth of the magnetic induction through-the-earth communication system decreases with the growth of soil moisture. When $SER_t \leq 10^{-3}$, as soil moisture rises from 0% to 75%, the achievable communication depth of BPSK modulation drops from about 336 m to roughly 213 m, while that of QPSK modulation reduces from around 347 m to approximately 206 m. This indicates that the reliability of the magnetic induction through-the-earth communication system deteriorates as soil moisture increases.

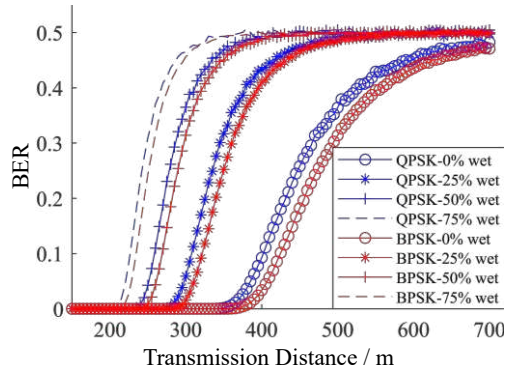


Fig 9 *Relationship between BER and communication distance of MI TTE communication system.*

To investigate the relationship between modulation order and transmission distance of magnetic induction through-the-earth channels under different formation medium conditions, Figure 10 presents the maximum available modulation orders for uncoded signals transmitted via QAM modulation in magnetic induction through-the-earth communication systems under various transmission distances and soil moisture contents, subject to the constraint $SER_t \leq 10^{-3}$.It can be observed from Figure 10 that 64-QAM can be adopted within a transmission distance of 160 m when the soil moisture is 0%. When the soil moisture is lower than 50%, 32-QAM is still applicable at 160 m. For a soil moisture of 75%, 8-QAM can be realized within 155 m.At short transmission distances, high-order modulation can be utilized to increase the data rate, i.e., improve the transmission efficiency of the through-the-earth communication system. However, the allowable modulation order declines with the growth of transmission distance or soil moisture. When the transmission distance becomes large, only BPSK modulation can be adopted to guarantee the communication reliability of the through-the-earth system.

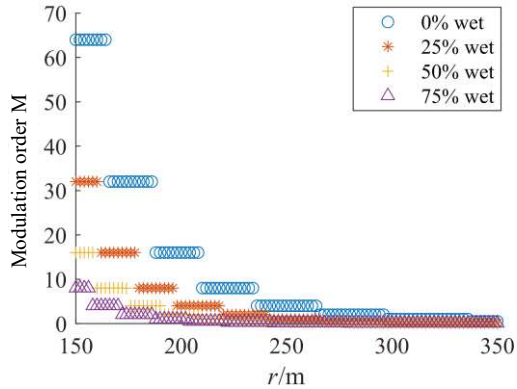


Fig 10 *Maximum modulation order of MI TTE communication system.*

Conclusion: This paper analyzes the channel and noise characteristics of MI-TTE communication for long-distance transmission scenarios. The main conclusions are summarized as follows:

(1) As the conductivity of the through-the-earth propagation medium increases, the magnitude of the channel transfer function $H(f)$ decreases correspondingly. Nevertheless, the resonant frequency corresponding to the maximum magnitude of $H(f)$ is barely affected by the propagation medium, which indicates that the transmission medium is not a dominant factor for carrier frequency configuration in MI-TTE communication systems.

(2) The noise captured by the receiver of MI-TTE communication is also shaped by the resonant loops. The noise amplitude reaches its peak at the resonant frequency and decays at frequencies far away from the resonance point. Compared with the amplitude spectrum of the useful received signal, the noise amplitude of the receiving loop decays much more slowly and exhibits a flatter profile.

(3) Subject to a given bit error rate constraint $SER_t \leq 10^{-3}$, the maximum communication depth of MI-TTE systems adopting the identical modulation scheme declines significantly with rising soil moisture. In other words, the communication reliability degrades as soil moisture increases.

(4) Under the BER constraint $SER_t \leq 10^{-3}$, the maximum modulation order of QAM supported by the MI-TTE system varies with different transmission distances and soil moisture contents. When the transmission distance or soil moisture is relatively low, high-order modulation can be employed to boost data transmission rate and improve communication efficiency. However, the allowable modulation order decreases as the propagation distance or soil moisture grows.

Author contributions : The model and scenario were proposed by M.Dai and W.Yang. The investigation and analysis were completed by Y.Wang and Y.Zhu. Writing, review, and editing were performed by C.Ma, H.Li and X.Jia. Project management and supervision were handled by B.Zhu, H.Cheng and L.Sun. All authors have read and agreed to the published version of the manuscript.

Funding: This work was supported by China National Coal Group Key Science and Technology Project (XJ2024088064), and Key Science and Technology Project of Ministry of Emergency Management of the People's Republic of China (2024EMST131302).

Data availability : All data generated or analyzed during this study are included in this published article.

Consent to publish: We certify that the submission is original work and has not been published previously and is not under consideration for publication elsewhere. Its publication is approved by all authors and tacitly or explicitly by the responsible authorities where the work was carried out. We also promise that if the submission is accepted, it will not be published elsewhere in the same form, in English or in any other language, without the written consent of the Publisher.

Competing interests: To the authors' best knowledge, there do not exist any competing interests in this work.

References

1. HU Qingsong, YANG Wei, DING Enjie, et al. State-of-the-art and trend of emergency rescue communication technologies for coal mine[J]. Journal on Communications, 2019, 40(5): 163－179.
2. ZHAO Haojiang, YANG Wei. An emergency rescue communication system and environmental monitoring subsystem for underground coal mine based on wireless mesh network[J]. International Journal of Distributed Sensor Networks,2018,14(10):1-20.
3. FU Tianhui, LIU Baoheng, WANG Yongbin. Review of research on through-the-earth wireless communication［J］. Science Technology and Engineering，2021，21(17) : 6993-7001.

4. JIA Yulong, LI Fengxia, TAO Jinyi, et al. Transmission characteristics of very low frequency electromagnetic wave of mine-seam wireless through-the-earth communication system[J]. Industry and Mine Automation,2015,41(9):31-33.
5. LIU Baoheng, FU Tianhui, HOU Wenda.Transmission distance analysis of wireless magnetic induction through-the-earth communication[J]. Tele communication Engineering,2022,62(03):361-366.
6. ZHANG Z, LIU E, Qu X, et al. Connectivity of Magnetic Induction-Based Ad Hoc Networks[J]. IEEE Transactions on Wireless Communications, 2017, 16(7): 4181-4191.
7. TANG Tongtong, YANG Wei, SHAO Xiaotao. Transmission attenuation characteristics of electromagnetic wave through irregular layered strata[J]. Journal of China Coal Socie-ty,2017,42(7):1912-1918.
8. PEPLINSKI N R, ULABY F T, DOBSON M C. Dielectric properties of soils in the 0.3-1.3-GHz range[J]. IEEE Trans. on Geoscience and Remote Sensing,1995,33(3):803-807.
9. KIM J Y, LEE H J, OH J H, et al. Magnetic Induction-Based Test-Bed System for Magnetic Communication in Underground Mines[C]//2023 20th Annual IEEE International Conference on Sensing, Communication, and Networking (SECON). IEEE, 2023: 388-389.
10. TIAN Wenlong, YANG Wei and SHAO Xiaotao. A High-Precision Magnetic Induction Through-the-Earth Positioning Scheme[J]. IEEE Access, 2021, 9: 35109-35120.
11. TIAN Wenlong, YANG Wei and SHAO Xiaotao. A high-precision long-distance magnetic induction through-the-earth positioning method[J]. Journal of Huazhong University of Science and Technology (Natural Science Edition),2021,49(12):99-104.
12. TIAN Wenlong, YANG Wei and SHAO Xiaotao. A High-Precision Dual-Frequency Magnetic Induction Through-the-Earth Positioning Method[J]. IEEE Access, 2021,.162325-162336.
13. SUN Z, AKYILDIZ I F. Magnetic induction communications for wireless underground sensor networks[J]. IEEE Trans. on Antennas and Propagation,2010,58(7):2426-2435.
14. KISSELEFF S, AKYILDIZ I F, GERSTACKER W. Digital signal transmission in magnetic induction based wireless underground sensor networks[J]. IEEE Transactions on Communications, 2015, 63(6): 2300-2311.
15. DAI Mengtian, YANG Wei. Analysis on channel capacity of magnetic induction based long-distance through-the-earth communication[J]. Chinese Journal of Radio Science, 2023, 38(3): 502－509.
16. AGBINYA J I. Principles of Inductive Near Field Communications for Internet of Things[M]. River Publishers, 2011.
17. KISSELEFF S, AKYILDIZ I F, GERSTACKER W. On modulation for magnetic induction based transmission in wireless underground sensor networks[C]//2014 IEEE International Conference on Communications (ICC). IEEE, 2014: 71-76.
18. ZHANG Y, ZHAO Z, Chen K. Frequency splitting analysis of magnetically-coupled resonant wireless power transfer[C]//2013 IEEE Energy Conversion Congress and Exposition. IEEE, 2013: 2227-2232.
19. KURS A, KARALIS A, MOFFATT R, et al. Wireless power transfer via strongly coupled magnetic resonances[J]. science, 2007, 317(5834): 83-86.
20. SCHLEGEL C, MALLAY M, TOUESNARD C. Atmospheric magnetic noise measurements in urban areas[J]. IEEE Magnetics Letters, 2014, 5:1-4.